THE JOURNAL OF BIOLOGICAL CHEMISTRY VOL. 285, NO. 17, pp. 12840–12850, April 23, 2010
Printed in the U.S.A.

The Anti-tumorigenic Properties of Peroxisomal Proliferator-activated Receptor α Are Arachidonic Acid Epoxygenase-mediated*[S]

Received for publication, November 2, 2009, and in revised form, January 29, 2010 Published, JBC Papers in Press, February 23, 2010, DOI 10.1074/jbc.M109.081554

Ambra Pozzi[‡§], Vlad Popescu[‡], Shilin Yang[‡], Shaojun Mei[‡], Mingjian Shi[‡], Satu M. Puolitaival[¶‖], Richard M. Caprioli[‖], and Jorge H. Capdevila[‡**1]**

*From the Departments of [‡]Medicine, [¶]Chemistry, and **Biochemistry and the [‖]Center for Mass Spectrometry Research, Vanderbilt University Medical School, Nashville, Tennessee 37232 and the [§]Veterans Affairs Hospital, Nashville, Tennessee 37212*

Prevalence and mortality make cancer a health challenge in need of effective and better tolerated therapeutic approaches, with tumor angiogenesis identified as a promising target for drug development. The epoxygenase products, the epoxyeicosatrienoic acids, are pro-angiogenic, and down-regulation of their biosynthesis by peroxisomal proliferator-activated receptor α (PPARα) ligands reduces tumor angiogenesis and growth. Endothelial cells lacking a Cyp2c44 epoxygenase, a PPARα target, show reduced proliferative and tubulogenic activities that are reversed by the enzyme's metabolites. In a mouse xenograft model of tumorigenesis, disruption of the host *Cyp2c44* gene causes marked reductions in tumor volume, mass, and vascularization. The relevance of these studies to human cancer is indicated by the demonstration that: (*a*) activation of human PPARα down-regulates endothelial cell CYP2C9 epoxygenase expression and blunts proliferation and tubulogenesis, (*b*) in a PPARα-humanized mouse model, activation of the receptor inhibits tumor angiogenesis and growth, and (*c*) the CYP2C9 epoxygenase is expressed in the vasculature of human tumors. The identification of anti-angiogenic/anti-tumorigenic properties of PPARα points to a role for the receptor and its epoxygenase regulatory target in the pathophysiology of cancer, and for its ligands as candidates for the development of a new generation of safer and better tolerated anti-cancer drugs.

Despite advances in diagnosis and treatment, cancer continues to pose major clinical challenges and is the focus of efforts to develop therapies that combine effectiveness with low toxicity. Among these, angiogenesis is a current target of attempts aimed to reduce tumor vascularization and growth (1, 2), because it holds a promise for more effective and better tolerated approaches for cancer treatment. The peroxisomal proliferator-activated nuclear receptors (PPARs),[2] *i.e.* PPARα, PPARγ, and PPARδ, control the transcription of genes mostly involved in the regulation of lipid metabolism and energy homeostasis. Although several roles for the PPARδ and -γ isotypes in the pathophysiology of cancer have been proposed (3–5), recent animal studies have identified PPARα ligands as effective inhibitors of tumor angiogenesis and growth (6–8). The potential significance of these findings has been emphasized by epidemiological data (9–12), and by studies in human cancer cell lines (13–16), suggesting that PPARα ligands such as Fenofibrate and Bezafibrate may have beneficial effects in the prognosis of human cancer. A unique feature of these PPARα ligands is that, through their long history of clinical use as hypolipidemic drugs, they have been shown to be well tolerated and to have limited side effects and/or toxicity, indicating that they could serve as targets for the development of novel, safer, and with low toxicity anti-cancer treatments.

The PPARα-mediated transcriptional regulation of members of the *CYP2C* gene subfamily of cytochrome P450s is well established (17, 18), as is the role of these enzymes in the metabolism and bio-activation of arachidonic acid (AA) (19). The CYP2C epoxygenases metabolize AA to 5,6-, 8,9-, 11,12-, and 14,15-epoxyeicosatrienoic acids (EETs) (19), and these metabolites have been characterized as pro-angiogenic lipids *in vitro* (20–22) and *in vivo* (23). The demonstration that the anti-tumorigenic effects of PPARα ligand activation were associated with reductions in the endothelial expression of the murine Cyp2c44 epoxygenase and in the levels of plasma and endothelial EETs (6), suggested pro-angiogenic and pro-tumorigenic roles for this epoxygenase, and pointed to this enzyme as a target of the anti-tumorigenic effects resulting from PPARα activation (6). The murine Cyp2c44 epoxygenase generates 11,12- and 14,15-EET as its major products (24), is expressed in endothelial cells (6), and is under PPARα transcriptional control (6). Similarly, human CYP2C8 and CYP2C9, catalytic homologues of murine Cyp2c44 (25), have been identified as endothelial epoxygenases (21, 22), and their participation in

* This work was supported, in whole or in part, by National Institutes of Health Grants DK 5P01-038226 and GM 5R01-037922 (to J. H. C.), DK R01-065123 (to A. P.), and GM 5R01-58008 (to R. M. C.). This work was also supported by a Department of Veterans Affairs Merit Award (to A. P.). Mass Spectrometric analyses were done with support from the Vanderbilt University Cancer Center Grant CA-68485.

[S] The on-line version of this article (available at http://www.jbc.org) contains supplemental Figs. 1–5 and Table 1.

[1] To whom correspondence should be addressed: Dept. of Medicine, Vanderbilt University Medical School, Medical Center North S-3223, Nashville, TN 37232. Tel.: 615-322-4968; Fax: 615-343-4704; E-mail: jorge.capdevila@vanderbilt.edu.

[2] The abbreviations used are: PPAR, peroxisomal proliferator-activated receptor; AA, arachidonic acid; Cyp2c44, CYP2C8, and CYP2C9, members of the cytochrome P450 gene family 2, subfamily C, mouse polypeptide 44, and human polypeptides 8 and 9, respectively; EET, epoxyeicosatrienoic acid; Wyeth, Wyeth-14,643; VEGF, vascular epidermal growth factor; VEGFR, VEGF receptor; MALDI, matrix-assisted laser desorption ionization; MAPK, mitogen-activated protein kinase; ERK, extracellular signal-regulated kinase; hPPARα, human PPARα.

VEGF-stimulated angiogenesis has been suggested (26). Furthermore, a role for the human CYP2J2 epoxygenase in the promotion of neoplastic phenotypes and metastasis has been proposed based on CYP450 overexpression and inhibitor studies (27, 28). Given the many biological activities attributed to the EETs (19, 29–31), the growing evidence of an involvement of AA epoxygenases in renal and vascular physiology, cell proliferation, and angiogenesis (29–31), there is increase interest in the identification and the development of tools to intervene in the biosynthesis and/or disposition of these lipid mediators (32, 33). This report: (*a*) identifies the murine *Cyp2c44* as a host pro-angiogenic and pro-tumorigenic epoxygenase gene, and the target of the anti-angiogenic and anti-tumorigenic effects of PPARα ligand activation, (*b*) characterizes the anti-angiogenic and anti-tumorigenic properties of human PPARα, and the CYP2C9 epoxygenase as its regulatory target, and (*c*) identifies CYP2C9 as a epoxygenase expressed in the vasculature of several human tumor samples.

EXPERIMENTAL PROCEDURES

All animal protocols were approved by the Vanderbilt University Medical Center Institutional Animal Care and Use Committee. Male (12–20 weeks old) wild-type (WT), *Cyp2c44*$^{-/-}$ (KO), and PPARα-humanized mice (*hPPARα*), all in isogenic *129SvJ* backgrounds, were fed commercial diets and allowed free access to water. Wyeth was administered in the drinking water as neutral 0.02% solution (v/v). Transgenic mice expressing the human PPARα gene in a murine PPARα null background (*hPPARα*) were a gift of Dr. Frank J. Gonzalez (NCI, National Institutes of Health, Bethesda, MD). *hPPARα* mice were generated by microinjection of a linearized PAC clone (Genome Systems, St. Louis, MO) containing the complete *hPPAR* gene, including ~100 and 28 kb of its 5′- and 3′-flanking sequences, respectively (34). Transgenic founders were bred with *PPARα*$^{-/-}$ mice, and hPPARα mice in mouse *PPARα*$^{-/-}$ backgrounds were further bred for at least 10 generations onto a *129SvJ* background. The expression of human PPARα in the *hPPARα* mice was periodically assessed by PCR amplification of tail DNAs as described (34).

Cyp2c44 Gene Disruption and Analyses of Primary Tumor Growth—Global *Cyp2c44* mouse knockouts were purchased from Lexicon Genetics Inc. (Texas), and derived from an Omnibank ES cell line (clone OST85045) in which, insertion of a viral gene trap at exon 4 of *Cyp2c44* (66 bp from the upstream intro/exon boundary) generates truncated, non-coding, Cyp2c44 transcripts. These animals were used to generate homozygous *Cyp2c44*$^{+/+}$ and *Cyp2c44*$^{-/-}$ mice in isogenic *129/SvJ* backgrounds (from the progeny of an F15 cross of heterozygous *Cyp2c44*$^{+/-}$ mice). Tail DNAs were genotype by PCR with primers flanking the trap insertion site (forward, 5′-caccttcatcctggcctgtg-3′; reversed, 5′-ttacgactgagccacattcc-3′), and a primer specific for the 3′-end of the viral trap (forward, 5′-ggcgttacttaagctagcttgc-3′). These primers amplify 360- and 350-bp fragments unique to the WT or the disrupted gene, respectively. For tumorigenesis studies, WT, KO, and hPPARα mice were given two dorsal subcutaneous injections of syngeneic murine p60.5 cells (3×10^5 cells in 200 μl of phosphate-buffered saline per site) (35). The animals were sacrificed 2 weeks after, and tumor volume, weight, and number were evaluated. Averaged tumor volumes were calculated using the following formula: tumor volume (mm^3) = (length [mm] × width $[mm]^2$)/2 (36).

Cell Culture and Assays—Pulmonary microvascular endothelial cells isolated from WT, KO, and *hPPARα* mice were cultured in EGM-2-MV (Clonetics) containing 5% fetal calf serum as described (35), and discarded after three passages. The large T antigen/ras/Myc-transformed mouse fibroblast cell line (p60.5 cell line) was cultured as described (35). Human dermal microvascular endothelial cells were obtained from Invitrogen and cultured as recommended. For the proliferation assay, cells were plated (5×10^3 cells/well; 96-well plate) in serum-free media alone or containing either: (*a*) VEGF (10–50 ng/ml), (*b*) 11,12-EET (1 μM), or (*c*) AA (5 μM). In some experiments, cells were cultured in serum-containing medium (2.5% final concentration) and in the absence or presence of different concentrations of Wyeth. Two days after, the medium was replaced with media containing [^{3}H]thymidine (1 μCi/well), the cells incubated for 48 h, and proliferation was determined as described before (35). In some experiments, the [^{3}H]thymidine assay was validated by quantifications of cell number. For the Matrigel-based tubulogenesis assay, capillary-like structure formation was analyzed as described (36, 37). Briefly, 96-well plates were coated with 50 μl of Matrigel and incubated for 30 min at 37 °C. Endothelial cells (1.5×10^4 cells/well) in serum-free media with or without EETs (1 μM, each), AA (5 μM), or VEGF (50 ng/ml), were plated over the solidified Matrigel. To determine the effects of Wyeth, cells were cultured in complete media with or without Wyeth (25 μM). After 4 days, the cells were serum-starved for 24 h, suspended in serum-free media with or without Wyeth (25 μM), and then plated over solidified Matrigel in the presence or absence of EETs (1 μM). The formation of capillary-like structures was recorded hourly for the next 10 h. Shown in the figures are representative images taken 6 h after plating. To quantify capillary-like network formation, cellular nodes were defined as junctions linking at least three cells (35), and counted from digital images. Three independent experiments were performed each time in triplicates, with a total of 36 images analyzed per treatment.

RNA Isolation and Analysis—Total RNAs were isolated with the TRIzol Reagent (Invitrogen) and reverse-transcribed using SuperScript II (Invitrogen), oligo$(dT)_{12-18}$, and a random primer mixture. For analysis of Cyp2c44 transcripts, reverse-transcribed products from mouse liver or from cultured endothelial cells were amplified using exon-specific PCR primers (supplemental Fig. 1). Analyses of Cyp2c44 or CYP2C9 expression were done by quantitative real-time PCR using the TaqMan Gene Expression Assay System (Applied Biosystems) and Cyp2c44- or CYP2C9-selective PCR primers. Gene expression was normalized based on the relative abundance of human or mouse β-actin transcripts.

Western Blot, Immunofluorescence, and Mass Spectral Imaging—For analyses of ERK1/2, Akt, or VEGFR2 activation, semi-confluent endothelial cells were serum-starved for 24 h and then incubated for 20 min with or without VEGF (50 ng/ml), AA (5 μM), or 11,12-EET (1 μM). Cells were then washed with phosphate-buffered saline, collected, and lysed,

and equal amounts of cell lysate (20 μg of protein/lane) were resolve by gel electrophoresis and transferred to Immobilon-P membranes. Western blots were performed using the following rabbit antibodies: anti-phospho ERK, anti-ERK, anti-phospho Akt anti-Akt (all from Cell Signaling Technologies), anti-phospho VEGFR2 (R&D), anti-mouse VEGFR2 (Abcam), anti-CYP2C23 (raised against recombinant rat CYP2C23), and a Cyp2c44 peptide antibody raised against the enzyme's IGRHQPPSMKDKMKC peptide (GenScript) (6). Analyses of immunoreactive proteins were done using peroxidase-conjugated secondary antibodies and an ECL kit (Amersham Biosciences). Phospho-VEGFR2, phospho-ERK, phospho-Akt, VEGFR2, ERK, and Akt bands were quantified by densitometry analysis, and signals were expressed as phospho-VEGFR2/VEGFR2, phospho-ERK/ERK, phospho-Akt/Akt ratios, respectively.

Frozen mouse tumor sections (7 μm each) were stained with rat anti-mouse CD31 antibody (1:400, BD Pharmingen), and/or rabbit anti-mouse Cyp2c44 (1:1000), followed by rhodamine-conjugated goat anti-rat IgG and/or fluorescein isothiocyanate-conjugated goat anti-rabbit (1:200, Jackson ImmunoResearch). The degree of vascularization, expressed as percentage of area occupied by CD31-positive structures/microscopic field, was evaluated using Scion Imaging Software (Frederick, MD) (35), using two images/tumor and ten tumors/genotype. Serial sections of a freshly frozen human clear cell renal cell carcinoma, human lung adenoma, or metastatic melanoma (7 μm each) were stained with hematoxylin and eosin for histological visualization, or co-stained with mouse anti-human CD31 and rabbit anti-human CYP2C9 antibodies, followed by fluorescein isothiocyanate-conjugated goat anti-rabbit and rhodamine-conjugated goat anti-mouse IgG antibodies (1:200).

For mass spectral imaging, serial sections of the renal carcinoma used for immunofluorescence (12 μm each) were thaw-mounted onto gold-coated MALDI plates, washed with ethanol (38), and stored ~2 h under vacuum. A robotic spotter (Portrait, LabCyte) was used to deposit in fifty cycles a solution of porcine trypsin (0.8 mg/ml) in 16 mM HOAc, 84 mM NH_4HCO_3 (one drop per cycle, fly-by mode) across the tissue section at a spot center-to-center spacing of 300 μm, followed by 30 cycles of 40 mg/ml 2,5-dihydroxybenzoic acid matrix in 50:50:0.1% (v/v) acetonitrile:water:trifluoroacetic acid. The digested sections were analyzed on an UltraFlex II MALDI time of flight mass spectrometer (Bruker Daltonics, Billerica, MA) in reflector mode, summing 4 × 100 laser shots (λ = 355 nm) per matrix spot. The spectra were smoothed and baseline-corrected using FlexAnalysis software. Mass spectral analysis of a trypsin digest of purified recombinant CYP2C9 identified diagnostic peptides at *m/z* 1491 (ANRGFGIVFSNGKK), 2415 (VQEEIERVIGR), and 3017 (YALLLLLKHPEVTAKVQ EEIERVIGR). Scanning was done at these diagnostic *m/z* values, and two-dimensional images were acquired, normalized, and visualized with FlexImaging (38).

Analysis and Quantification of Epoxygenase Metabolites—To determine the effect of VEGF on endothelial cell EET biosynthesis, 24-h serum-starved wild-type endothelial cells were incubated with VEGF (10 ng/ml) in serum-free medium. After 24 h, the cells were incubated with AA (10 μM), and after 3 h they were processed as reported (6, 23, 39). The EETs and dihydroxy eicosatrienoic acids present in endothelial cells or plasma from untreated or Wyeth (0.02% in drinking water) treated mice were extracted, purified, and quantified by the isotope ratio method (39) using Ultra high pressure liquid chromatography/tandem mass spectrometry. Biological samples were extracted in the presence of equimolar mixtures of $^2H_3$-labeled EETs and $^2H_8$-labeled dihydroxy eicosatrienoic acids (5 ng each).

Statistical Analysis—Two-tail Student's *t* test was used for group comparisons, and for the analysis of variance using Sigma-Stat software for statistical differences between multiple groups. $p \leq 0.05$ was considered statistically significant.

RESULTS AND DISCUSSION

The down- and up-regulation of VEGF and thrombospondin, respectively (7), or reductions in the expression of the murine Cyp2c44 epoxygenase and biosynthesis of pro-angiogenic EETs (6) were proposed as the mechanisms responsible for the anti-tumorigenic effects of PPARα ligands. To characterize the roles of the Cyp2c44 epoxygenase in endothelial cell function, tumor angiogenesis, and growth, and to define its value as a potential therapeutic target, we generated colonies of *Cyp2c44*$^{-/-}$ (KO) and wild type (WT) mice in isogenic *129/SvJ* backgrounds as described under "Experimental Procedures." The KO mice reproduce and develop normally and lack outward symptoms of disease or organ malfunction. As shown under the supplemental materials, only in DNAs from KO mice we detect the presence of a diagnostic, viral trap-derived, 350-bp fragment (supplemental Fig. 1*A*). Furthermore, while RNAs from WT endothelial cells (supplemental Fig. 1, *B–D*) and liver (supplemental Fig. 1, *E* and *F*) contain Cyp2c44 coding transcripts, those from KO animals contain truncated, nonfunctional, transcripts encoding exons 1 to 3 (supplemental Fig. 1, *B*, *E*, and *F*).

Contribution of Plasma Lipoprotein Uptake and/or Endothelial Biosynthesis to the Pool of Pro-angiogenic EETs—The EETs circulate bound to plasma lipoproteins (40), and lipoprotein uptake is a known source of endothelial lipids. Furthermore, the liver is a source of plasma, lipoprotein-bound, EETs (19), and PPARα ligands down-regulate hepatic Cyp2c expression and reduce plasma EET levels (6, 17–19). To characterize the origin of the pro-angiogenic EETs (plasma lipoprotein uptake or endogenous endothelial biosynthesis), and the organ target of the anti-tumorigenic responses resulting from PPARα activation, we compared the effects of Wyeth 14,643 (Wyeth) (6), a PPARα-selective ligand (17, 18, 34), in the levels of EETs present in the plasma of WT and KO mice. Disruption of *Cyp2c44* did not significantly change the levels of plasma EETs, and Wyeth reduced their plasma concentrations in a *Cyp2c44* genotype-independent fashion; with only minor changes in isomeric composition (supplemental Table 1), indicating that its effects are associated with changes in the expression of alternate hepatic epoxygenase isoforms. Based on these results, we concluded that Cyp2c44 plays a limited role in regulating plasma EET levels, that plasma uptake does not contribute to the pool of endothelial EETs, and that the endothelial Cyp2c44 epoxygenase is likely the source of endothelial EETs (6). These

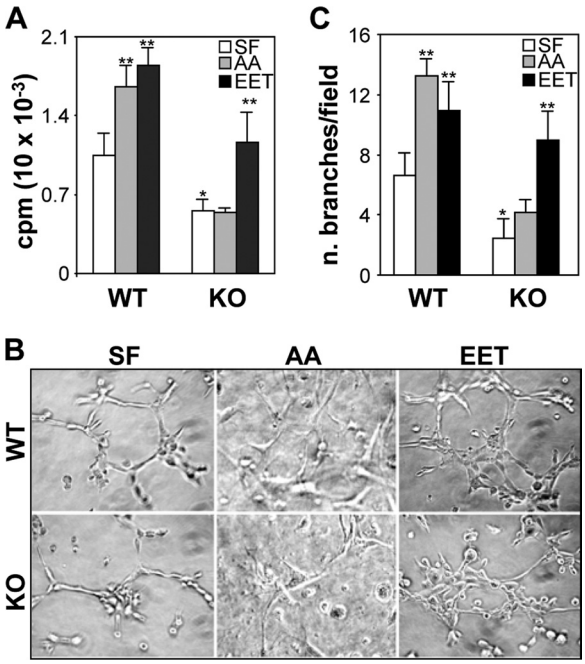

FIGURE 1. **The Cyp2c44 epoxygenase mediates the basal and AA-stimulated proliferative and tubulogenic activities of endothelial cells.** Primary cultures of lung endothelial cells from wild-type (*WT*) and *Cyp2c44*$^{-/-}$ (*KO*) mice in serum-free media (*SF*) or in serum-free media containing arachidonic acid (*AA*) (5 μM) or 11,12-EET (*EET*) (1 μM) were: *A*, cultured 48 h prior to the addition of [^{3}H]thymidine (0.1 μCi/well) and then their proliferation quantified as described under "Experimental Procedures." Values are averages ± S.D. calculated from three experiments, each performed in quadruplicates. * and ** indicate significant differences ($p < 0.05$) between untreated or treated WT and KO cells, respectively; *B* and *C*, plated onto Matrigel and the formation of tube-like structures analyzed by light microscopy. *B*, representative images of capillary like structures taken 6 h after plating. *C*, capillary network formation was quantified as described under "Experimental Procedures," and the values are averages ± S.D. of branch number per microscope field, calculated from three experiments each performed in triplicates. * and ** are as in *A*.

conclusions are supported by published studies showing that cultured mouse lung microvascular endothelial cells express Cyp2c44 and biosynthesize EETs (6, 23). Nonetheless, after several attempts we were unable to reproducibly quantify the EETs present in the KO endothelial cells, because, if present, their levels were below the detection sensitivity of our mass spectrometry techniques.

The Cyp2c44 Epoxygenase Is a Component of the Akt and MAPK Kinase-mediated Proliferative and Tubulogenic Responses of Endothelial Cells to AA and VEGF—Pro-angiogenic functions have been proposed for the human and rodent CYP2C epoxygenases and their metabolites (6, 8, 20–23). However, the identity of the relevant CYP2C isoform and the role in angiogenesis *in vivo* remain to be defined. To study the role played by the endothelial Cyp2c44 epoxygenase in basal and agonist-stimulated angiogenesis, we compared the proliferative and tubulogenic activities of primary pulmonary endothelial cells from WT and KO mice cultured in serum-free media in the presence or absence of AA. AA has been shown to increase endothelial EET biosynthesis by ~3.5-fold (23). Compared with WT cells, and under non-stimulated conditions, the KO cells show significantly reduced growth rates (Fig. 1*A*); a phenotype that became evident during culture; with KO cells consistently reaching confluence in approximately double the time of WT cells. A role for the Cyp2c44 epoxygenase in AA-stimulated cell growth was indicated by the observation that, although WT cells respond to AA (the Cyp2c44 epoxygenase substrate, and precursor of EET biosynthesis) (24) by increasing proliferation, the KO cells are unable to do so (Fig. 1*A*). When plated on Matrigel, WT endothelial cells generate tube-like structures (37), an activity indicative of angiogenic potential, and nearly doubled upon the addition of AA (Fig. 1, *B* and *C*). In contrast, the tubulogenic capacity of the KO cells was markedly reduced whether in the presence or absence of added AA (Fig. 1, *B* and *C*). Because AA is also a precursor for the synthesis of pro-angiogenic prostanoids or hydroxy acids (41–43), the role of the Cyp2c44 epoxygenase on the effects described for AA, was establish in phenotype rescue experiments in which we compared the proliferative and tubulogenic responses of WT and KO cells to the epoxygenase 11,12-EET metabolite (24). As seen in Fig. 1*A*, the addition of 11,12-EET to the KO endothelial cells restored their proliferative activity to levels comparable to those of untreated WT cells. Similarly, 11,12-EET restored the tubulogenic capacity of KO cells to levels that were slightly higher than those seen in untreated WT cells (Fig. 1, *B* and *C*). Interestingly: (*a*) WT and KO endothelial cells cultured in serum-free media maintain basal, albeit low, proliferative and tubulogenic activities (Fig. 1, *A* and *C*), perhaps the result of basal, non-Cyp2c44-catalyzed EET biosynthesis, or limited contributions from prostanoids and/or hydroxy acids (41–43), and (*b*) while 11,12-EET rescued the growth and tubulogenic phenotypes of KO endothelial cells, its effects on KO cells were slightly lower to those on untreated WT cells, perhaps reflecting functional differences between the endogenous EETs and those added exogenously.

Based on the above studies, it was concluded that the: (*a*) Cyp2c44 epoxygenase is the predominant pro-angiogenic epoxygenase in mouse pulmonary endothelial cells, (*b*) Cyp2c44 epoxygenase is required for optimal basal or AA-stimulated endothelial cell proliferation and tubulogenesis, (*c*) reductions in growth and tubulogenesis seen in the *Cyp2c44* KO cells are due to reductions in the biosynthesis of pro-angiogenic EETs, and (*d*) pro-angiogenic roles of the Cyp2c44 epoxygenase are AA-dependent and EET-mediated. These EET effects on endothelial cell function raise important questions regarding the mechanism(s) by which these lipids promote angiogenesis. Although this is yet to be established, likely candidates are: (*a*) signaling through a membrane-bound EET receptor, (*b*) direct effects on intracellular kinases, or (*c*) participation in growth factor mediated signaling (26, 44, 45). In this regard, EETs cross cell membranes efficiently and are found as esters of intracellular glycerophospholipids (19, 40), plasma membrane-bound EET receptors are yet to be unequivocally identified (46), and there is no evidence for direct EET effects on protein kinases.

VEGF and its receptors (VEGFRs) are common targets of anti-angiogenic therapies for cancer treatment (47–49). However, most anti-VEGF approaches suffer from unwanted effects, including hypertension, azotemia, impaired wound healing, and the development of resistance (50–53), and there is a need for more effective and safer methods to intervene in tumor angiogenesis. Several *in vitro* studies suggested a role for

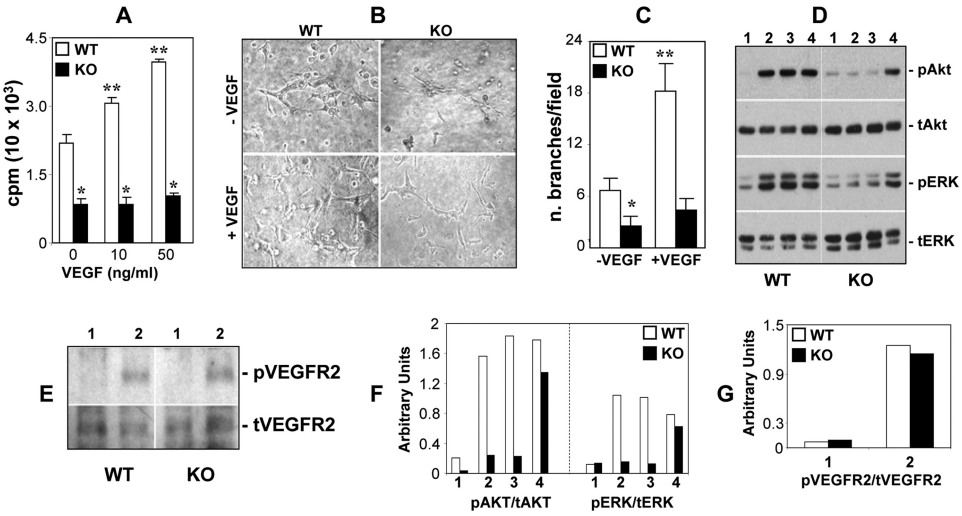

FIGURE 2. **The Cyp2c44 epoxygenase is a component of VEGF-stimulated angiogenic pathways.** WT and KO endothelial cells were: *A*, cultured in SF medium with or without the indicated VEGF concentrations and proliferation determined as described under "Experimental Procedures." Values are averages ± S.D. calculated from three experiments performed in quadruplicates. * and ** are as in Fig. 1*A*. *B* and *C*, plated onto Matrigel in SF medium with or without VEGF (50 ng/ml). *B*, representative images of capillary-like structures taken 6 h after plating. *C*, capillary network formation was quantified as described under "Experimental Procedures," and the values are averages ± S.D. of branch number per microscope field, calculated from three experiments each performed in triplicates. * and ** are as in Fig. 1*A*. *D* and *E*, serum starved for 24 h and then treated with vehicle, VEGF (50 ng/ml), AA (5 μM), or 11,12-EET (1 μM) (*lanes 1*, *2*, *3*, and *4*, respectively) for 20 min, and an equal amount of cell lysate protein (20 μg/lane) was analyzed by Western blot for levels of activated and total ERK and Akt (*D*), or activated and total VEGR2 (*E*). *Vertical lines* indicate non-adjacent gel *lanes*. *F* and *G*, pAkt, tAkt, pERK, tERK, pVEGFR2, and tVEGFR2 bands were quantified by densitometry analysis, and the signal was expressed as a pAkt/tAkt (*F*), pERK/tERK (*F*), and pVEGFR2/tVEGFR2 (*G*) ratio. Values are the mean of two experiments that differ from the mean by <20%.

the CYP2C epoxygenases and the EETs in VEGF signaling and/or expression (26, 45, 54), and for VEGF in CYP2C epoxygenase expression (22). In agreement with this, serum-starved WT endothelial cells incubated in the presence of AA respond to VEGF treatment with a 2.4-fold increase in cellular EET biosynthesis (from 0.17 ± 0.03 to 0.41 ± 0.03 ng of EET/mg of cell protein, for control and VEGF-treated cells, respectively; n = 3). To characterize the role played by the endothelial Cyp2c44 epoxygenase in VEGF-mediated angiogenesis, we compared the proliferative and tubulogenic responses of WT and KO endothelial cells to VEGF. As shown in Fig. 2*A*, VEGF stimulated the proliferation of WT endothelial cells in a dose-dependent fashion, with a doubling in DNA [^{3}H]thymidine incorporation at ~50 ng/ml. Similarly, at 50 ng/ml, VEGF increased the tubulogenic activity of WT cells by nearly 3-fold (Fig. 2, *B* and *C*) but, under similar conditions, failed to stimulate the proliferation (Fig. 2*A*) and tubulogenesis (Fig. 2, *B* and *C*) of cells lacking Cyp2c44 epoxygenase activity. Wyeth has been shown to reduce endothelial cell Cyp2c44 expression and EET biosynthesis by 50–80% (6). To determine whether Cyp2c44 is the major and/or only epoxygenase involved in endothelial cell functions, we compared the proliferative responses of WT and KO cells to Wyeth. In contrast to WT cells, the addition of increasing concentrations of Wyeth to KO endothelial cells did not alter their growth properties (supplemental Fig. 2), showing that Cyp2c44 is a major functional target for Wyeth, and that the ligand effects on endothelial cell proliferation are Cyp2c44 epoxygenase-mediated.

The activation of the ERK1/2 and Akt kinase pathways in endothelial cells by the EETs, and the finding that inhibition of the upstream MAPK/ERK kinase and phosphatidylinositol 3-kinase kinases abrogates the proliferative and tubulogenic responses to EETs have been reported (6, 8, 20–23). To determine the role of the Cyp2c44 epoxygenase in MAPK activation, as well as possible mechanisms by which this enzyme and its metabolites stimulate proliferation and tubulogenesis, we compared the effects of AA, VEGF, and 11,12-EET on ERK1/2 and Akt activation in WT and KO endothelial cells. As shown in Fig. 2 (*D* and *F*), VEGF and AA are equally effective in activating ERK1/2 and Akt phosphorylation in WT cells, but they fail to do so in KO cells. On the other hand, 11,12-EET activates both cellular kinases in a genotype-independent fashion (Fig. 2, *D* and *F*), indicating that the effects of AA and VEGF are Cyp2c4 epoxygenase- and EET-mediated. Analysis of VEGFR2 phosphorylation shows that VEGF stimulates equally the activation of this receptor subtype in WT and KO endothelial cells (Fig. 2, *E* and *G*), showing that this process is Cyp2c44 epoxygenase-independent. The demonstration that VEGF stimulates mitogenic and tubulogenic activity only in WT cells, and that its effects on MAPK and Akt phosphorylation are impaired in *Cyp2c44* null cells, identifies this epoxygenase as a component of VEGF-mediated signaling that ultimately leads to increased angiogenesis (45). Moreover, these studies also indicate that the MAPK and Akt activation responses elicited by 11,12-EET are either VEGFR2-independent or involve events downstream from this receptor.

Tumor Vascularization and Growth Are Blunted and PPARα-ligand Independent in Mice Carrying a Disrupted Cyp2c44 Gene—We and others have demonstrated that the administration of PPARα ligands to mice decreases tumor growth and vascularization (6–8) and attributed these responses to the effects of these ligands on endothelial Cyp2c44 expression and EET biosynthesis (6). Having documented the participation of the Cyp2c44 epoxygenase in endothelial cell function and VEGF signaling, we sought to investigate whether this epoxygenase played an *in vivo* role as: (*a*) target for the anti-tumorigenic effects of PPARα ligand activation and (*b*) a host pro-angiogenic and pro-tumorigenic enzyme. To address these important issues, groups of WT and KO mice were left untreated or administered Wyeth (0.02% v/v) in their drinking water. Two days later, all animals received two subcutaneous injections with syngeneic murine p60.5 cells (35), and then, the administration of Wyeth to the treated group was continued for the duration of the experiment. Two weeks after the cell injections, all animals were sacrificed, and their tumor load was quantified by measurements of tumor number, weight, and vol-

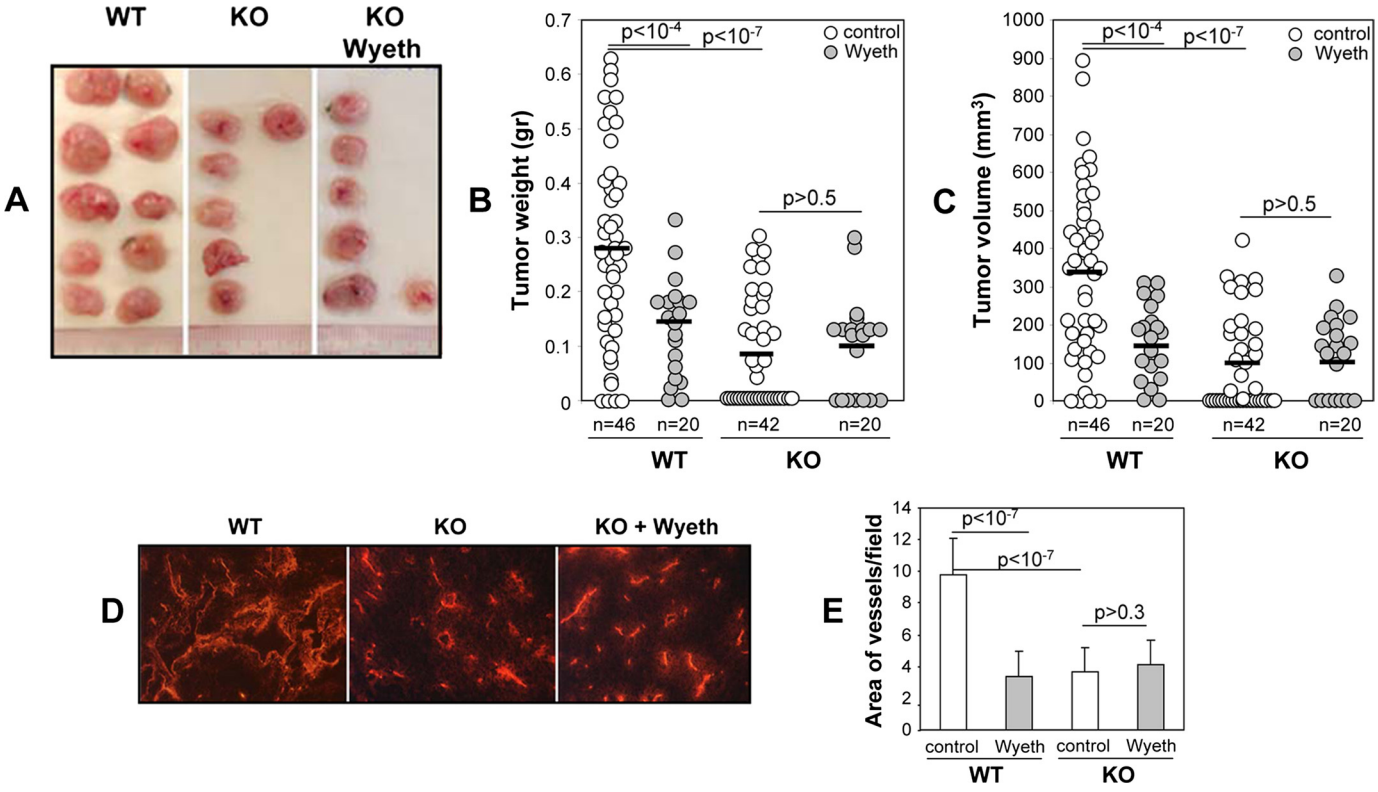

FIGURE 3. **The Cyp2c44 epoxygenase regulates tumor growth and angiogenesis.** Groups of WT and *Cyp2c44*$^{-/-}$ (*KO*) mice were either left untreated of administered Wyeth (0.02%, v/v) in their drinking water for 2 days prior to receiving two subcutaneous injections with p60.5 cells. Wyeth treatment was continued for the next 2 weeks, at which point mice were sacrificed, and their tumor load quantified. *A*, representative images of tumors grown in untreated WT and KO mice, and in Wyeth-treated KO mice. *B* and *C*, quantification of the weight (*B*) and volume (*C*) of the tumors grown in untreated and Wyeth-treated WT and KO mice. *Circles* show individual tumor values, *while bars* show mean values. *D* and *E*, frozen sections of tumors from untreated WT and KO mice, and from Wyeth-treated KO mice were stained with anti-mouse CD31 antibodies (*D*), and their degrees of vascularization quantified as percent of the area occupied by CD31-positive structures per microscopic field (*E*). The values in *E* are averages ± S.D. calculated from ten tumors/group with two images analyzed per tumor.

ume. To confirm the efficacy of the Wyeth treatment regime, and because liver hypertrophy is a documented consequence of PPARα ligand activation in rodents (18, 34, 55, 56), we compared changes in liver size (as percent of body weight) resulting from the administration of Wyeth, and showed that the organs in both Wyeth-treated WT and KO groups were 1.5- to 1.7-fold bigger than those in untreated mice (supplemental Fig. 3*A*).

A role for the host *Cyp2c44* epoxygenase gene in tumor initiation was indicated by the fact that, although 96% of WT mice ($n = 23$) developed tumors, only 76% of the KO mice ($n = 21$) did so ($p < 0.03$). Moreover, nearly 87% of the WT mice *versus* 28% of the KO mice developed two tumors ($p < 1.7E-05$). Visual inspections showed that, compared with WT, the tumors in KO mice were smaller, pale, and less vascularized (Fig. 3*A*). Measurements of tumor weight (Fig. 3*B*) and volume (Fig. 3*C*) confirmed that lack of a host *Cyp2c44* gene leads to substantial reductions in tumor mass (Fig. 3*B*) and volume (Fig. 3*C*). Immunofluorescence analysis of endothelial CD31 expression showed that, at difference with the WT, tumors in the KO mice showed less and more diffuse CD31-associated fluorescence, indicative of reduced vascularization (Fig. 3, *D* and *E*). Thus, the effects of *Cyp2c44* gene disruption on tumor mass, volume, and vascularization are similar to those resulting from the administration of Wyeth to WT mice (6). Importantly, at difference with its effects on WT animals (6), Wyeth had minimal or no effects on the size (Fig. 3*B*), volume (Fig. 3*C*), and/or vascularization of the tumors grown in KO mice (Fig. 3, *D* and *E*), showing that its anti-tumorigenic effects were Cyp2c44-dependent and not associated with changes in the expression of alternate murine epoxygenases and/or non-epoxygenase pathways (7, 41–43). Lastly, to confirm that Wyeth decreases *in vivo* endothelial Cyp2c44 expression, tumor sections from untreated and Wyeth-treated mice were co-stained with anti-CD31 and anti-Cyp2c44 antibodies and submitted to immunofluorescence analysis. Tumors grown in untreated WT mice show vascular Cyp2c44 immunoreactivity, that is significantly decreased in Wyeth-treated animals, and absent in both Wyeth-treated or untreated KO mice (supplemental Fig. 4). Taken together, these results demonstrate that: (*a*) the host *Cyp2c44* epoxygenase functions as a pro-angiogenic and pro-tumorigenic gene; (*b*) impaired angiogenesis is a causative component of the anti-tumorigenic effects associated with *Cyp2c44* gene disruption; and (*c*) the Cyp2c44 epoxygenase is a target of the anti-tumorigenic effects resulting from PPARα ligand activation. The key role played by the host endothelial epoxygenase in these tumorigenic responses was corroborated by the demonstration that cultured transformed p60.5 cells do not biosynthesize EETs, nor proliferate in response to EETs (6). The generality of the above conclusions is supported by studies with different mice strains and tumor cell lines showing direct correlations between PPARα-mediated reductions in endothelial Cyp2c44 expression and tumor angiogenesis and growth (6, 8).

Activation of Human PPARα Inhibits Endothelial Cell Proliferation and Tubulogenesis—Efforts to extrapolate results obtained in mouse models with PPARα ligands to the pathophysiology of human cancer are hindered by known differences between humans and rodents in PPARα signaling (34, 55, 56). Thus, sustained activation of the rodent PPARα causes liver hypertrophy and, after prolonged exposure, hepatocarcinoma (18, 34, 55, 56); effects that are absent in humans, even after prolonged exposure to the PPARα ligands used for the treatment of dyslipidemias. To begin addressing the relevance of our studies to the pathophysiology of human cancer, and initiate the validation of PPARα ligands as inhibitors of human tumor vascularization and growth, we first analyzed the effects of Wyeth on the growth and tubulogenic properties of cultured human microvascular endothelial cells. The CYP2C8 and CYP2C9 isoforms have been identified as the major human CYP2C epoxygenase expressed in kidney (25) and endothelium (21, 22), respectively, and their participation in VEGF signaling (26), and roles in the migration and tubulogenesis of cultured human endothelial cell are published (20–22). Incubation of human endothelial cells with increasing concentrations of Wyeth showed that the ligand blocks cell proliferation in a dose-dependent fashion, with its maximum effects between 25 and 100 μM Wyeth (Fig. 4*A*). Next, to investigate the role of the CYP2C9 epoxygenase in the proliferative and tubulogenic responses of human endothelial cells to Wyeth, we incubated cells in the presence of either serum, serum containing Wyeth, or serum containing a mixture of Wyeth and 11,12-EET or Wyeth and 14,15-EET (1 μM each), and measured proliferation and tubulogenesis as described under "Experimental Procedures." At 25 μM, Wyeth reduced by nearly 70% the proliferative and tubulogenic activities of these cells (Fig. 4, *B–D*), and its effects were accompanied by a down-regulation in CYP2C9 mRNA levels (Fig. 4*E*) and 31–40% reductions in overall EET biosynthesis. A role for the CYP2C9 epoxygenase in the above responses to Wyeth was indicated by the fact that 11,12- and 14,15-EET, both products of the CYP2C9 epoxygenase (25), restored the proliferative and tubulogenic activities of Wyeth-treated cells to levels similar (Fig. 4*B*) or significantly higher (Fig. 4, *D* and *C*) to those observed in untreated WT cells.

Activation of the Human PPARα in PPARα-humanized Mice Inhibits Tumor Vascularization and Growth—The development of a PPARα-humanized mouse (hPPARα) model in which the human *PPARα* gene, containing coding and regulatory sequences, was introduce onto a mouse *PPARα* null background (34), has allowed *in vivo* comparisons of the responses of the human and mouse receptors to ligand activation (34, 55, 56). These studies demonstrate that activation of rodent, but not human PPARα, by ligands such as Fenofibrate or Wyeth alters *let-7c* expression and c-Myc protein levels, leading to hepatomegaly and liver carcinoma (34, 55). Importantly, *hPPARα* mice do not develop liver hypertrophy or carcinoma, even after prolonged exposure to PPARα ligands (34, 56).

To investigate the anti-tumorigenic properties of the human PPARα receptor, groups of WT and *hPPARα* mice were left as untreated controls, or administered Wyeth (0.02% v/v) in their drinking water. Two days after, all mice received two subcutaneous injections of syngenic murine p60.5 cells, and the treatment of the Wyeth group was continued for the duration of the experiment. Two weeks after the cell injections, the animals were sacrificed, and their tumor load quantified by measure-

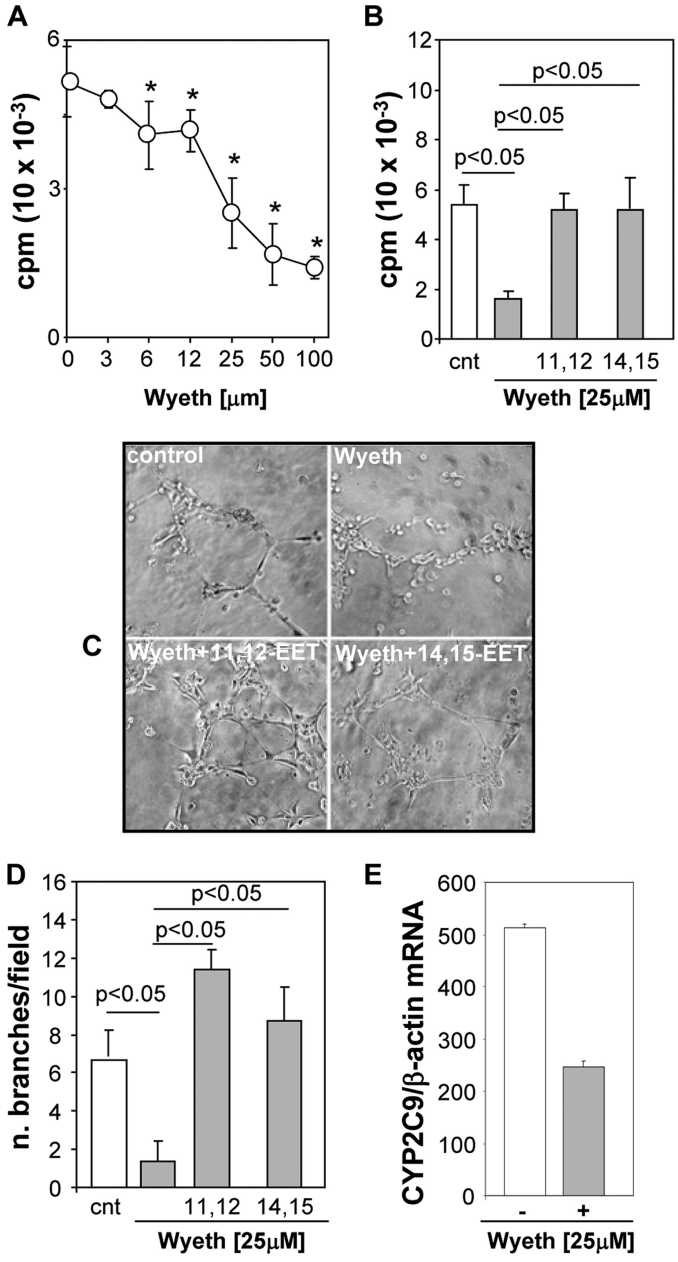

FIGURE 4. **Wyeth inhibits the proliferative and tubulogenic activities of human endothelial cells.** Human microvascular endothelial cells were: *A*, cultured in medium containing 2.5% fetal calf serum without Wyeth, or with Wyeth added at the indicated concentrations, and their proliferation was determined as described under "Experimental Procedures." Values are averages ± S.D. of three experiments performed in quadruplicates. *, significant differences ($p < 0.05$) between untreated and Wyeth-treated cells. *B*, cultured in media containing 2.5% fetal calf serum (*cnt*) with or without Wyeth (25 μM) or a mixture of Wyeth (25 μM) and 11,12-EET or 14,15-EET (1 μM each), and their proliferation determined as above. *C* and *D*, plated onto Matrigel in SF medium (*cnt*) with or without Wyeth (25 μM) or a mixture of Wyeth (25 μM) and 11,12-EET or 14,15-EET (1 μM each). *C*, representative images of capillary-like structures taken 6 h after plating. *D*, capillary network formation was quantified as described under "Experimental Procedures," and the values are averages ± S.D. of branches per microscope field calculated from three experiments each performed in triplicates. *E*, the levels of CYP2C9 mRNA in untreated and Wyeth-treated cells were analyzed by quantitative real-time PCR and normalized using the β-actin mRNA as reference. Values are averages ± S.D. calculated from six determinations done with reverse-transcribed products from two different experiments.

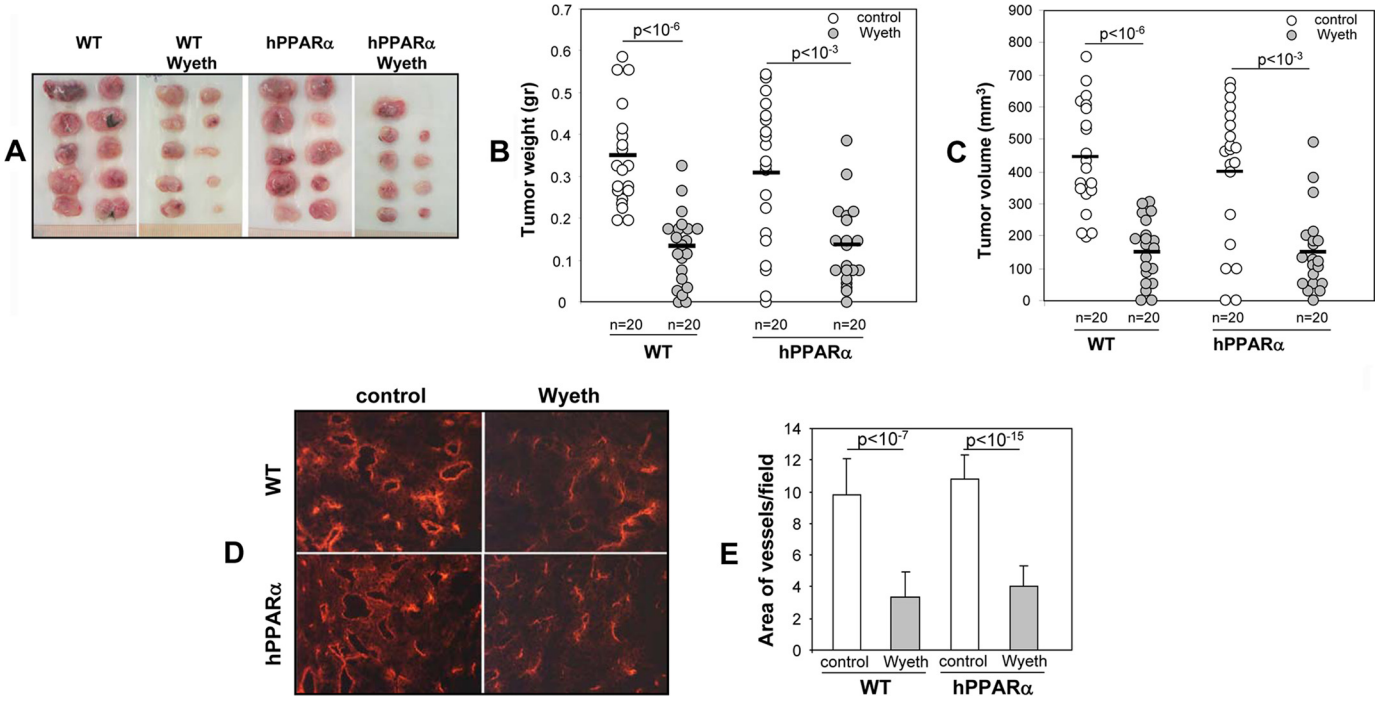

FIGURE 5. **Ligand activation of human PPARα in PPARα humanized (hPPARα) mice blunts tumor angiogenesis and growth.** Groups of WT and *hPPARα* mice were either left untreated or administered Wyeth (0.02%, v/v) in their drinking water for 2 days prior to receiving two subcutaneous injections with p60.5 cells. Wyeth treatment was continued for the next 2 weeks, at which point mice were sacrificed, and their tumor load was quantified. *A*, representative images of tumors grown in untreated and Wyeth-treated WT and hPPARα mice. *B* and *C*, quantification of the weight (*B*) and volume (*C*) of tumors grown in untreated and Wyeth-treated WT and *hPPARα* mice. *Circles* show individual tumor values, whereas *bars* show mean values. *D* and *E*, frozen sections of tumors from untreated (control) and Wyeth-treated (*Wyeth*) WT and *hPPARα* mice were stained with anti-mouse CD31 antibodies (*D*), and their degrees of vascularization was quantified as the percentage of the area occupied by CD31-positive structures per microscopic field (*E*). The values in *panel E* are averages ± S.D. calculated from ten tumors/group with two images analyzed per tumor.

ments of tumor number, weight, and volume. Although Wyeth caused liver hypertrophy in WT mice (6), the ligand had no significant effects on the livers of the *hPPAR* animals (34) (supplemental Fig. 3). A comparison of the effects of Wyeth on the tumorigenic responses of the rodent and human PPARα receptors shows that: (*a*) there are no significant differences between untreated WT and *hPPARα* mice in tumor numbers, mass or volume (Fig. 5, *A*, *B*, and *C*, respectively), (*b*) as is the case with WT mice, the activation of the human PPARα receptor by Wyeth leads to marked reductions in tumor number, mass, and volume (Fig. 5, *A*, *B*, and *C*, respectively), and (*c*) for both WT and *hPPARα* mice, the anti-tumorigenic effects of Wyeth are linked to reduction in vascularization (Fig. 5, *D* and *E*) and in expression of endothelium-associated Cyp2c44 epoxygenase (supplemental Fig. 4). These results indicate that the anti-tumorigenic effects of hPPRAα ligand activation involve reduced vascular Cyp2c44 epoxygenase expression and, as a consequence, decreased tumor angiogenesis and growth. Consistent with this finding, treatment of *hPPARα* primary endothelial cells with Wyeth causes dose-dependent reductions in cell proliferation, that are similar to those observed with WT cells (supplemental Fig. 5).

In summary, these studies show that the anti-tumorigenic effects of Wyeth are PPARα species-independent and associated with reductions in the expression of an endothelial epoxygenase (6) and that PPARα ligand activation could serve as a novel and potentially effective target for the development of low toxicity anti-angiogenic cancer therapies. In this regard, preliminary experiments show that Fenofibrate, a PPARα ligand in clinical use, is as effective as Wyeth in reducing human endothelial cell proliferation and tubulogenesis (not shown).

Human CYP2C9 Is a Tumor Epoxygenase Expressed in the Tumor-associated Vasculature—The endothelial expression of the human CYP2C8 and CYP2C9 epoxygenases and their *in vitro* roles in angiogenesis has been reported (21, 22). However, although the relative contributions of these isoforms to the biosynthesis of pro-angiogenic EETs remain undetermined, the studies summarized above point to CYP2C9 as a pro-angiogenic epoxygenase and a potential target for the anti-tumorigenic effects of ligand activated human PPARα. Therefore, to further document the relevance of our mouse studies to human cancer, we utilized mass spectrometry imaging techniques (38) to identify and map the expression and distribution of CYP2C9 in a human clear cell renal carcinoma. This type of carcinoma was selected for these studies, because its frozen sections retain most of their morphological details after *in situ* proteolysis. As shown in Fig. 6*A*, under light microscopy, the stained sections of the renal carcinoma show tumor-free and tumor-containing areas. Although the left portion contains tissue of normal appearance, the center and right portions are dominated by tumor-containing tissue, with a predominance of tumor dense nodules near the boundary between normal and tumor tissue. To unequivocally establish whether or not the CYP2C9 epoxygenase is a tumor-expressed enzyme, and to determine whether its expression levels are associated with gradients in tumor density, serial sections of the renal carcinoma were submitted to *in*

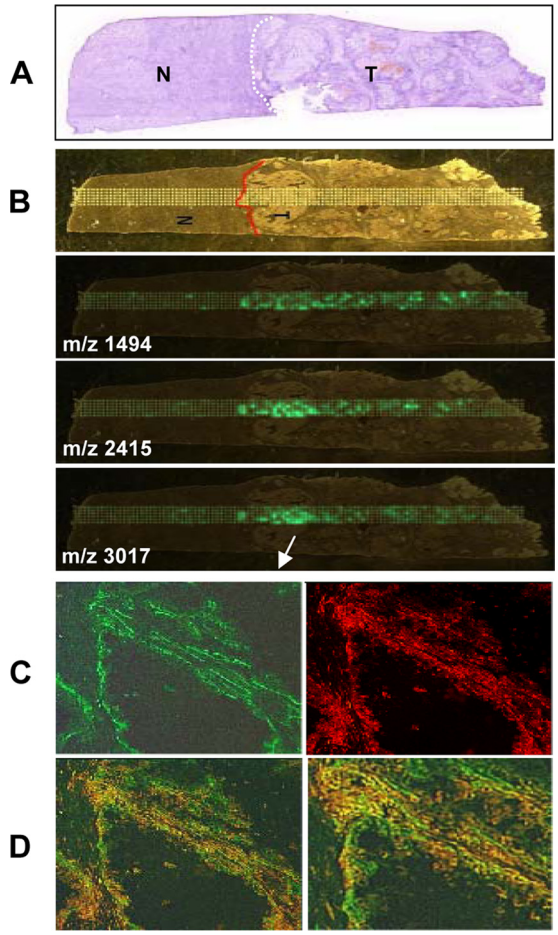

FIGURE 6. **Mass spectral identification of CYP2C9 as a tumor-expressed human epoxygenase.** *A* and *B*, frozen serial sections of a human clear renal cell carcinoma were stained with either hematoxylin & eosin for evaluation of tumor-free (*N*) and tumor-containing (*T*) areas (*A*) or co-stained with anti-human CYP2C9 (*red*) and anti-human CD31 (*green*) to visualize the localization of CYP2C9 (*C*). *D*, overlay *images* show the expression of CYP2C9 epoxygenase in the tumor-associated vasculature. *B*, trypsin-digested serial sections of the human cell carcinoma shown in *A* were analyzed by mass spectral imaging at *m/z* 1491, 2415, and 3017, diagnostic for CYP2C9. Laser sampling was done using the *dot matrix* shown superimposed to a light microscopy image of the sections. CYP2C9-positive regions are identified by co-localization of mass signals derived from the CYP2C9 diagnostic peptides shown in *green*.

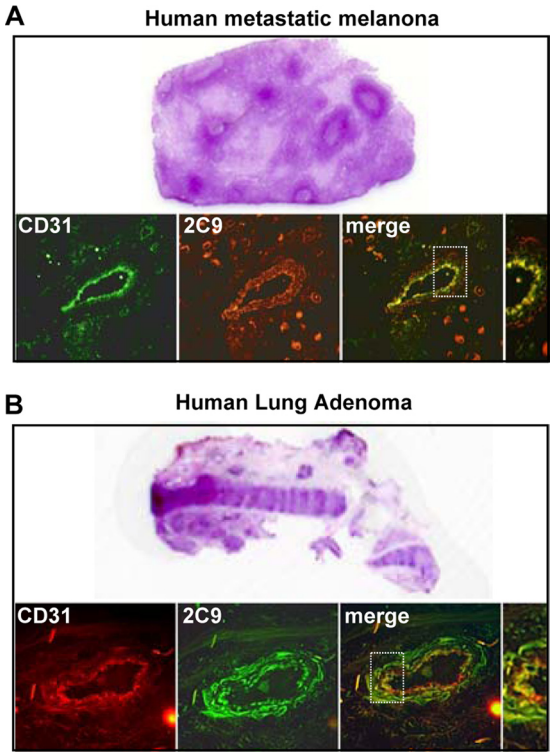

FIGURE 7. **Vascular expression of the CYP2C9 epoxygenase in human tumors.** *A*, frozen serial sections of a human lymph node with metastatic melanoma were stained with hematoxylin & eosin for evaluation of metastasis or exposed to anti-human CYP2C9 (*red*) or anti-human CD31 (*green*) antibodies to visualize CYP2C9 expression and vascular structures. *Overlay images* reveal expression of the CYP2C9 epoxygenase in tumor-associated vasculature. *B*, frozen serial sections of a human lung adenoma were stained with hematoxylin & eosin, or co-stained with anti-human CYP2C9 (*green*) and anti-human CD31 (*red*) to visualize CYP2C9 expression and vascular structures. *Overlay images* reveal expression of CYP2C9 epoxygenase in tumor-associated vasculature.

situ trypsin digestion, and the distribution of CYP2C9-derived peptides analyzed by MALDI time of flight mass spectrometry by two-dimensional sampling as illustrated by the *dot sampling matrix* in Fig. 6*B*. Trypsin digestion of purified recombinant CYP2C9 yielded diagnostic peptides at *m/z* 1494, 2415, and 3017 and, therefore, imaging was done by mass monitoring at those *m/z* values. The *top frame* in Fig. 6 (Fig. 6*B*) shows a non-stained image of a section like those used for mass spectrometry and illustrates a distribution of tumor and tumor-free areas. The two dimensional laser-assisted scanning of these sections shows: (*a*) the spatial co-localization of mass signals originating from the CYP2C9-diagnostic peptides in the tumor-containing areas (Fig. 6, *A* and *B*), (*b*) that CYP2C9 is nearly undetectable in tumor free areas (Fig. 6, *A* and *B*), and (*c*) that the spatial distribution of CYP2C9 expression gradients coincides with the spatial distribution of tumor density, *i.e.* higher levels of expression in the middle tumor-dense region, and clear decreases in signal intensity as the scanning laser progressed to either the left or right of the center (Fig. 6, *A* and *B*). Importantly, a similar mass spectral imaging analysis of CYP2C8 diagnostic peptides failed to identify the presence of this epoxygenase in the renal carcinoma sections. Immunofluorescence analysis of the tumor-rich areas showed the presence of anti-CYP2C9 immunoreactive protein in anti-CD31-positive vessels (Fig. 6*C*), and the overlay of anti-CYP2C9 and anti-CD31 associated fluorescence identifies the co-expression of these proteins in the tumor vasculature (Fig. 6*D*). This mass spectral demonstration of a tumor-selective expression of the human CYP2C9 epoxygenase, and its immunofluorescence-based localization to the tumor vasculature, identifies this protein as a tumor-associated epoxygenase, and provides substantial support to the idea that this enzyme is responsible for the biosynthesis of pro-angiogenic EETs and involved in human tumor growth. Finally, to confirm the generality of these observations, we performed immunological analyses of CYP2C9 and CD31 expression in sections of a human metastatic melanoma and a human lung adenoma. Immunofluorescence analysis of tumor enriched areas in these sections, shows the presence of immunoreactive CYP2C9 epoxygenase and CD31-positive vascular structures in both samples (Figs. 7, *A* and *B*). Moreover, the superimposition of CD31- and CYP2C9-associated fluores-

cence confirmed that the epoxygenase and the endothelial cell marker are co-localized in the tumor vasculature (Fig. 7, *A* and *B*).

Most anti-cancer therapies interfere with tumor cell growth and propagation by disrupting intermediary metabolism and/or DNA replication, or by taking advantage of their distinct immunological properties. In contrast, angiogenesis-based approaches aim to reduce host-mediated angiogenesis and thus, tumor growth. The *in vivo* studies summarized here identify the host *Cyp2c44* gene as pro-tumorigenic and characterizes the key role played by its epoxygenase product in tumor angiogenesis and growth. Additionally, they identify the Cyp2c44 epoxygenase as a target for the anti-angiogenic and anti-tumorigenic effects resulting from the administration of Wyeth to tumor bearing mice (6–8). Notably, the demonstration that the human CYP2C9 epoxygenase is expressed in the tumor-associated vasculature, and that activation of the human PPARα receptor inhibits tumor angiogenesis and growth, suggests that maneuvers destined to down-regulate and/or inhibit CYP2C9 expression (*i.e.* PPARα ligand activation) or epoxygenase activity (*i.e.* CYP2C9 inhibition) could serve as targets for the development of novel anti-angiogenic, anti-tumorigenic therapies. In this regard, PPARα ligands are of special interest, because several of them have a long history of clinical use as hypolipidemic drugs, and they have proven to be safe and well tolerated (57, 58).

Finally, the identification of a role for the EETs in tumor angiogenesis and growth raises important questions regarding long term risks that may be associated with current efforts to use inhibitors of EET metabolism as anti-hypertensive, anti-inflammatory drugs (32, 33), particularly because inhibition of EET hydration could potentiate their mitogenic and tumorigenic activities (23, 44). Additionally, and equally important, these studies raise important questions regarding unknown/unforeseen pathological consequences that genetic, environmental, or chemical factors may have in the regulation of endothelial epoxygenase expression or EET concentrations, particularly in the pathophysiology of human cancer. In this regard, this study introduces a paradigm shift that could influence our views of the roles played by the P450 enzyme system in cancer therapy, from that of vehicles for anti-cancer drug disposition and/or activation, to that of active participants in the pathophysiology of tumor growth and cancer. It is expected that these studies will stimulate efforts to: (*a*) develop novel, CYP2C-based inhibitors of tumor angiogenesis and (*b*) consider during drug evaluation the physiological and/or pathophysiological consequences of interfering with the activity and/or expression of P450s involved in endogenous metabolic pathways.

Acknowledgments—We thank Dr. Frank Gonzalez (NCI, NIH) for providing the hPPARα mouse model and Dr. Pierre Massion for providing sections of human lung adenomas.

REFERENCES

1. Folkman, J. (2006) *Annu. Rev. Med.* **57,** 1–18
2. Folkman, J. (2007) *Nat. Rev. Drug Discov.* **6,** 273–286
3. Wu, C. W., Yu, J., and Sung, J. J. (2009) *Oncol. Rep.* **22,** 451–457
4. Ondrey, F. (2009) *Clin. Cancer Res.* **15,** 2–8
5. Wang, D., and Dubois, R. N. (2008) *PPAR Res.* **2008,** 931074
6. Pozzi, A., Ibanez, M. R., Gatica, A. E., Yang, S., Wei, S., Mei, S., Falck, J. R., and Capdevila, J. H. (2007) *J. Biol. Chem.* **282,** 17685–17695
7. Panigrahy, D., Kaipainen, A., Huang, S., Butterfield, C. E., Barnés, C. M., Fannon, M., Laforme, A. M., Chaponis, D. M., Folkman, J., and Kieran, M. W. (2008) *Proc. Natl. Acad. Sci. U.S.A.* **105,** 985–990
8. Pozzi, A., and Capdevila, J. H. (2008) *PPAR Res.* **2008,** 906542
9. Dellavalle, R. P., Drake, A., Graber, M., Heilig, L. F., Hester, E. J., Johnson, K. R., McNealy, K., and Schilling, L. (2005) *Cochrane Database Syst. Rev.*, CD003697
10. Tenenbaum, A., Boyko, V., Fisman, E. Z., Goldenberg, I., Adler, Y., Feinberg, M. S., Motro, M., Tanne, D., Shemesh, J., Schwammenthal, E., and Behar, S. (2008) *Cardiovasc. Diabetol.* **7,** 18
11. Steinhoff, M., Beyer, M., Roewert-Huber, J., Lukowsky, A., Assaf, C., and Sterry, W. (2008) *J. Am. Acad. Dermatol.* **58,** S88–S91
12. Golembesky, A. K., Gammon, M. D., North, K. E., Bensen, J. T., Schroeder, J. C., Teitelbaum, S. L., Neugut, A. I., and Santella, R. M. (2008) *Carcinogenesis* **29,** 1944–1949
13. Tsubouchi, Y., Sano, H., Kawahito, Y., Mukai, S., Yamada, R., Kohno, M., Inoue, K., Hla, T., and Kondo, M. (2000) *Biochem. Biophys. Res. Commun.* **270,** 400–405
14. Strakova, N., Ehrmann, J., Bartos, J., Malikova, J., Dolezel, J., and Kolar, Z. (2005) *Neoplasma* **52,** 126–136
15. Grabacka, M., Plonka, P. M., Urbanska, K., and Reiss, K. (2006) *Clin. Cancer Res.* **12,** 3028–3036
16. Urbanska, K., Pannizzo, P., Grabacka, M., Croul, S., Del Valle, L., Khalili, K., and Reiss, K. (2008) *Int. J. Cancer* **123,** 1015–1024
17. Savas, U., Griffin, K. J., and Johnson, E. F. (1999) *Mol. Pharmacol.* **56,** 851–857
18. Corton, J. C., Fan, L. Q., Brown, S., Anderson, S. P., Bocos, C., Cattley, R. C., Mode, A., and Gustafsson, J. Å. (1998) *Mol. Pharmacol.* **54,** 463–473
19. Capdevila, J. H., and Falck, J. R. (2002) *Prostaglandins Other Lipid Mediat.* **68–69,** 325–344
20. Medhora, M., Daniels, J., Mundey, K., Fisslthaler, B., Busse, R., Jacobs, E. R., and Harder, D. R. (2003) *Am. J. Physiol. Heart Circ Physiol.* **284,** H215–H224
21. Michaelis, U. R., Fisslthaler, B., Medhora, M., Harder, D., Fleming, I., and Busse, R. (2003) *FASEB J.* **17,** 770–772
22. Fleming, I., and Busse, R. (2006) *Hypertension* **47,** 629–633
23. Pozzi, A., Macias-Perez, I., Abair, T., Wei, S., Su, Y., Zent, R., Falck, J. R., and Capdevila, J. H. (2005) *J. Biol. Chem.* **280,** 27138–27146
24. DeLozier, T. C., Tsao, C. C., Coulter, S. J., Foley, J., Bradbury, J. A., Zeldin, D. C., and Goldstein, J. A. (2004) *J. Pharmacol. Exp. Ther.* **310,** 845–854
25. Zeldin, D. C., DuBois, R. N., Falck, J. R., and Capdevila, J. H. (1995) *Arch. Biochem. Biophys.* **322,** 76–86
26. Webler, A. C., Michaelis, U. R., Popp, R., Barbosa-Sicard, E., Murugan, A., Falck, J. R., Fisslthaler, B., and Fleming, I. (2008) *Am. J. Physiol. Cell Physiol* **295,** C1292–C1301
27. Jiang, J. G., Chen, C. L., Card, J. W., Yang, S., Chen, J. X., Fu, X. N., Ning, Y. G., Xiao, X., Zeldin, D. C., and Wang, D. W. (2005) *Cancer Res.* **65,** 4707–4715
28. Jiang, J. G., Ning, Y. G., Chen, C., Ma, D., Liu, Z. J., Yang, S., Zhou, J., Xiao, X., Zhang, X. A., Edin, M. L., Card, J. W., Wang, J., Zeldin, D. C., and Wang, D. W. (2007) *Cancer Res.* **67,** 6665–6674
29. Gauthier, K. M., Yang, W., Gross, G. J., and Campbell, W. B. (2007) *J. Cardiovasc. Pharmacol.* **50,** 601–608
30. Spector, A. A., and Norris, A. W. (2007) *Am. J. Physiol. Cell Physiol.* **292,** C996–C1012
31. Capdevila, J. H., Falck, J. R., and Imig, J. D. (2007) *Kidney Int.* **72,** 683–689
32. Chiamvimonvat, N., Ho, C. M., Tsai, H. J., and Hammock, B. D. (2007) *J. Cardiovasc. Pharmacol.* **50,** 225–237
33. Schmelzer, K. R., Kubala, L., Newman, J. W., Kim, I. H., Eiserich, J. P., and Hammock, B. D. (2005) *Proc. Natl. Acad. Sci. U.S.A.* **102,** 9772–9777
34. Yang, Q., Nagano, T., Shah, Y., Cheung, C., Ito, S., and Gonzalez, F. J. (2008) *Toxicol. Sci.* **101,** 132–139
35. Pozzi, A., Moberg, P. E., Miles, L. A., Wagner, S., Soloway, P., and Gardner, H. A. (2000) *Proc. Natl. Acad. Sci. U.S.A.* **97,** 2202–2207

36. Chen, X., Su, Y., Fingleton, B., Acuff, H., Matrisian, L. M., Zent, R., and Pozzi, A. (2005) *Int. J. Cancer* **116,** 52–61
37. Kubota, Y., Kleinman, H. K., Martin, G. R., and Lawley, T. J. (1988) *J. Cell Biol.* **107,** 1589–1598
38. Hardesty, W. M., and Caprioli, R. M. (2008) *Anal. Bioanal. Chem.* **391,** 899–903
39. Capdevila, J. H., Dishman, E., Karara, A., and Falck, J. R. (1991) *Methods Enzymol.* **206,** 441–453
40. Karara, A., Wei, S., Spady, D., Swift, L., Capdevila, J. H., and Falck, J. R. (1992) *Biochem. Biophys. Res. Commun.* **182,** 1320–1325
41. Nie, D., Tang, K., Diglio, C., and Honn, K. V. (2000) *Blood* **95,** 2304–2311
42. Kamiyama, M., Pozzi, A., Yang, L., DeBusk, L. M., Breyer, R. M., and Lin, P. C. (2006) *Oncogene* **25,** 7019–7028
43. Rao, R., Redha, R., Macias-Perez, I., Su, Y., Hao, C., Zent, R., Breyer, M. D., and Pozzi, A. (2007) *J. Biol. Chem.* **282,** 16959–16968
44. Chen, J. K., Capdevila, J., and Harris, R. C. (2002) *Proc. Natl. Acad. Sci. U.S.A.* **99,** 6029–6034
45. Yang, S., Wei, S., Pozzi, A., and Capdevila, J. H. (2009) *Arch Biochem. Biophys* **489,** 82–91
46. Yang, W., Tuniki, V. R., Anjaiah, S., Falck, J. R., Hillard, C. J., and Campbell, W. B. (2008) *J. Pharmacol. Exp. Ther.* **324,** 1019–1027
47. Press, M. F., and Lenz, H. J. (2007) *Drugs* **67,** 2045–2075
48. Veeravagu, A., Hsu, A. R., Cai, W., Hou, L. C., Tse, V. C., and Chen, X. (2007) *Recent Pat. Anticancer Drug Discov.* **2,** 59–71
49. Kuhn, H., Hammerschmidt, S., and Wirtz, H. (2007) *Curr. Med. Chem.* **14,** 3157–3165
50. Fernando, N. T., Koch, M., Rothrock, C., Gollogly, L. K., D'Amore, P. A., Ryeom, S., and Yoon, S. S. (2008) *Clin. Cancer Res.* **14,** 1529–1539
51. Sivanandam, V. G., Stephen, S. L., Hernandez-Alcoceba, R., Alzuguren, P., Zabala, M., van Rooijen, N., Qian, C., Berger, I., Gross, M. L., Prieto, J., and Kochanek, S. (2008) *J. Gene Med.* **10,** 1083–1091
52. Obhrai, J. S., Patel, T. V., and Humphreys, B. D. (2008) *Kidney Int.* **74,** 685–686
53. Chung, E. K., and Stadler, W. M. (2008) *Clin. Genitourin Cancer* **6,** S22–S28
54. Cheranov, S. Y., Karpurapu, M., Wang, D., Zhang, B., Venema, R. C., and Rao, G. N. (2008) *Blood* **111,** 5581–5591
55. Shah, Y. M., Morimura, K., Yang, Q., Tanabe, T., Takagi, M., and Gonzalez, F. J. (2007) *Mol. Cell. Biol.* **27,** 4238–4247
56. Gonzalez, F. J., and Shah, Y. M. (2008) *Toxicology* **246,** 2–8
57. Roberts, W. C. (1989) *Cardiology* **76,** 169–179
58. Rubins, H. B., Robins, S. J., Collins, D., Fye, C. L., Anderson, J. W., Elam, M. B., Faas, F. H., Linares, E., Schaefer, E. J., Schectman, G., Wilt, T. J., and Wittes, J. (1999) *N. Engl. J. Med.* **341,** 410–418